Twinned Crystals of Enantiomorphous Morphology of Racemic Alanine Induced by Optically Resolved α-Amino Acids; A Stereochemical Probe for the Early Stages of Crystal Nucleation†

Isabelle Weissbuch,* Ivan Kuzmenko, Madeleine Vaida, Sigal Zait,
Leslie Leiserowitz,* and Meir Lahav*

Department of Materials and Interfaces, The Weizmann Institute of Science 76100, Rehovot, Israel

Received March 1, 1994. Revised Manuscript Received May 2, 1994®

Crystallization of *R*,*S*-alanine in the presence of small amounts of other resolved α-amino acids results in the precipitation of the racemic compound as twinned crystals displaying a propeller-like morphology of 222 symmetry, in contrast to needlelike crystals of *mm*2 symmetry when grown from pure aqueous solution. This unusual twinning is explained by assuming that the supersaturated solutions contain ordered clusters of structures akin to the mature crystals of (*R*,*S*)-, (*R*)-, and (*S*)-alanine. The resolved α-amino acid additive, e.g., *R*′, stereospecifically inhibits growth of the *R*,*S* and *R* nuclei but not of the *S* nuclei. The latter serve as a template onto which the (*R*,*S*) crystals nucleate and grow. A model which takes into consideration the structural similarity between the racemic and chiral resolved forms of alanine to explain the twinning is presented. An X-ray diffraction analysis of a twinned crystal specimen is in agreement with a gradual change in structure, from a chiral crystal of space group $P2_12_12_1$ to the racemic compound of space group $Pna2_1$. To substantiate the model, crystals of alanine were grown from optically enriched solutions containing excess of one of the alanine enantiomers, which also induce the twinning phenomenon and an overall reduction in crystal symmetry. The relevance of these observations to the early stages of crystal nucleation is discussed.

Introduction

Crystal nucleation plays a paramount role in determining the physical and chemical properties of materials. Yet understanding and controlling the dynamics of the early stages of self-aggregation of molecules *en route* to crystal formation are still at a rudimentary stage. In the absence, to date, of general analytical tools to monitor, *in situ*, the structural changes of the embryonic species, indirect methods have still to be applied.

We adopt a logical working hypothesis that at the onset of crystallization nuclei form structures akin to that of the mature crystal. The strength of this simple assumption is that one may utilize known structural information stored in the grown crystal for the design of auxiliary molecules which can be stereospecifically targeted at those nuclei with arrangements similar to that of the mature crystal, and so prevent their eventual growth. This hypothesis has been successfully applied for the resolution of enantiomers which form conglomerates on crystallization,[1,2] for the induced growth of metastable crystalline polymorphs,[3] and for the oriented crystallization of glycine at the air-aqueous solution interface, in the presence of chiral resolved α-amino acids.[4]

The same procedure may be applied for the resolution of enantiomers that prefer to precipitate as racemic crystals provided there is not too large an energy gap and difference in solubility between the two phases. The auxiliary molecules must inhibit nucleation of the racemic as well as one of the enantiomorphous crystals. For such systems, the general approach for the crystallization of a particular phase, can be represented as follows. In a supersaturated solution containing a racemic mixture of *R*- and *S*-molecules one may anticipate the formation of a variety of nuclei among which are those with structures akin to the corresponding mature crystalline phases of the racemic compound (*R*,*S*), and the enantiomorphous (*R*) and (*S*) forms (Scheme 1). A chiral auxiliary, say *R*′, is designed such that on addition to the solution it will enantioselectively bind to {*R*,*S*} and {*R*} nuclei but not to the {*S*} nuclei. While adsorbed on the surfaces of those nuclei, the additive will prevent their further growth. Since we may expect that the *R*′ additives do not stereospecifically bind to the {*S*} nuclei, the latter will grow unperturbed and eventually precipitate.

This methodology was successfully applied for the induced optical resolution of (*R*,*S*)-histidine·HCl.[5] Ap-

---

† The paper is dedicated to the memory of Peggy Etter, whose untimely death has deprived the community of solid-state chemists of one of its leading figures. We present a piece of work that embodies elements that were close to her scientific interests on crystal nucleation and hydrogen bonding.

® Abstract published in *Advance ACS Abstracts*, August 15, 1994.

(1) Addadi, L.; Weinstein, S.; Gati, E.; Weissbuch, I.; Lahav, M. *J. Am. Chem. Soc.* 1982, *104*, 4610.

(2) Zbaida, D.; Weissbuch, I.; Shavit-Gati, E.; Addadi, L.; Leiserowitz, L.; Lahav, M. *React. Polym.* 1987, *6*, 241.

(3) Staab, E.; Addadi, L.; Leiserowitz, L.; Lahav, M. *Adv. Mater.* 1990, *2*, 40.

(4) Weissbuch, I.; Frolow, F.; Addadi, L.; Lahav, M.; Leiserowitz, L. *J. Am. Chem. Soc.* 1990, *112*, 7718.

(5) Weissbuch, I.; Zbaida, D.; Addadi, L.; Lahav, M.; Leiserowitz, L. *J. Am. Chem. Soc.* 1987, *109*, 1869.

0897-4756/94/2806-1258$04.50/0

Scheme 1

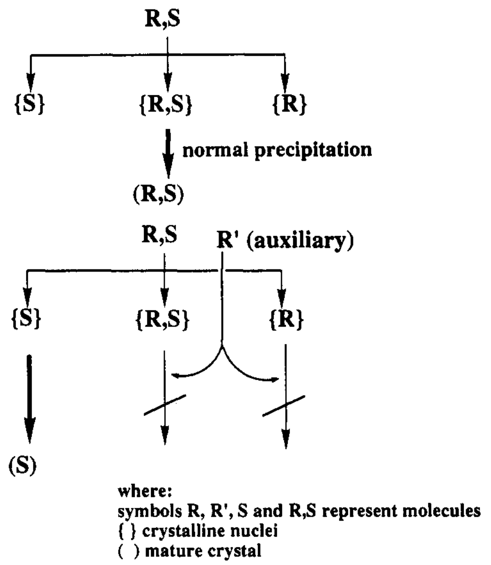

where:
symbols R, R', S and R,S represent molecules
{ } crystalline nuclei
( ) mature crystal

plying this approach for (*R*,*S*)-alanine resulted, however, in an unusual twinning[6-8] of the racemic compound displaying a propeller morphology, instead of precipitation of the chiral enantiomorph.

Here we describe a model that explains the formation of these twinned crystals by taking into account the similarity in structure of racemic and chiral alanine coupled with the enantioselective role played by the chiral additives. Furthermore, the twinning process also provided information on the structure of the molecular aggregate involved in the nucleation process.

Experimental Section

All α-amino acids were commercial analytical grade materials and they were used without further purification.

Crystallization Experiments. (*R*,*S*)-Alanine crystals were grown by slow evaporation of racemic aqueous solutions of concentration 25 g/100 mL, either pure or in the presence of 1–5 wt % optically pure or racemic α-amino acid additives such as phenylalanine, threonine, leucine. Series of crystals were grown from supersaturated solutions containing *R*:*S* (or *S*:*R*) alanine ratios varying from 40:60 to 0:100. In general the crystals were collected after 1-2 days. The crystals grown in the presence of additive or from solutions of 40:60 (*R*:*S* or *S*:*R*) alanine composition always displayed twinning.

Scanning Electron Microscopy. Crystals were first coated with gold and then mounted into the scanning electron microscope (SEM).

X-ray Diffraction Measurements. Crystallographic measurements were performed on a four-circle Rigaku single-crystal diffractometer using Cu Kα radiation from an 18-kW rotating anode X-ray generator. The X-ray beam was filtered with a graphite monochromator. The structure was refined using SHELXL-92 software.

Gas Chromatography. Enantiomeric composition of various alanine crystals was determined using a Hewlett-Packard 5890 gas chromatograph equipped with a 25-mm fused silica Chirasil-S-valine capillary column (purchased from Compack) at 95 °C, and 10 psi column head pressure with carrier gas (He) and FID detection. To get a volatile material, alanine crystals were derivatized as the *N*-(trifluoacetyl)alanine isopropyl ester.[9]

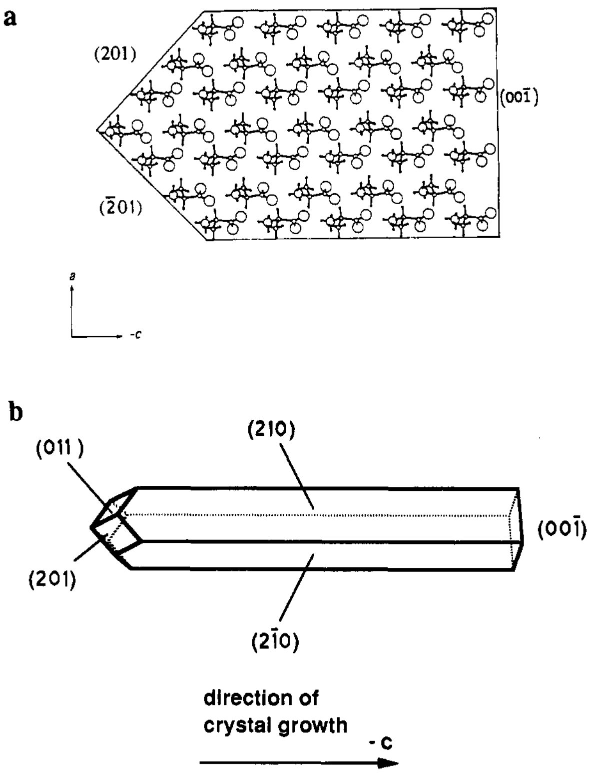

Figure 1. (a) Packing arrangement of (*R*,*S*)-alanine viewed along the *b* direction as delineated by the crystal faces. Note that the top and bottom horizontal lines are the intersections between the (210) and (2$\bar{1}$0) and ($\bar{2}$10) and ($\bar{2}\bar{1}$0) planes. (b) Computer-drawn morphology of the (*R*,*S*)-alanine crystals. Note that in some crystals {101} capped faces were observed instead of {201}.

Results and Discussion

Crystallization of (*R*,*S*)-Alanine. (*R*,*S*)-Alanine crystallizes from water in the orthorhombic polar space group $Pna2_1$ (a = 12.06 Å, b = 6.05 Å, c = 5.82 Å).[10] The crystals, which are needlelike in the *c* direction, are delineated by four symmetry-related side faces {210}, a "flat face" at one end of the polar *c* axis and "capped faces" at the opposite end (Figure 1). Thus the crystals exhibit morphological symmetry *mm*2, in keeping with the space group $Pna2_1$. The absolute structure of the crystal *vis-a-vis* its polar morphology was assigned using two independent methods. We performed experiments in the presence of additives that selectively inhibited growth at each of the two opposite poles of the crystal[11] and enantioselectively etched the {210} side faces of the crystal during initial stages of dissolution.[12] By these means we found that the molecules are arranged such that the NH_3^+ groups emerge at the "capped end" of the crystal and so the CO_2^- groups at the end terminated by a "flat face". The direction from the "capped end" to the "flat face" was arbitrarily denoted as $-c$, and so the "flat face" was indexed (00$\bar{1}$) (Figure 1). We had also shown that in aqueous solutions pure (*R*,*S*)-alanine crystals grow unidirectionally, via a "relay" type mechanism, along the polar axis at the (00$\bar{1}$) face which exposes the carboxylate groups.[13] The crystals barely grow in the opposite $+c$ direction at which end the amino groups

---

[6] Cahn, R. W. *Adv. Phys. Q. Suppl. Philos. Mag.* **1954**, *3*, 12.

[7] Gay, P. *The Crystalline State, An Introduction*; Oliver and Boyd: Edinburgh, 1972.

[8] Klapper, H. *Prog. Cryst. Growth Charact.* **1987**, *14*, 367.

[9] Konig, W. A. *The Practice of Enantiomer Separation by Capillary Gas Chromatography*; Huthig: Heidelberg, 1987; p 20.

[10] Donohue , J. *J. Am. Chem. Soc.* **1950**, *72*, 949.

[11] Wolf, J. M.Sc. Thesis, Feinberg Graduate School, 1986.

[12] Shimon, L. J. W.; Wireko, F. C.; Wolf, J.; Weissbuch, I.; Addadi, L.; Berkovitch-Yellin, Z.; Lahav, M.; Leiserowitz, L. *Mol. Cryst. Liq. Cryst.* **1986**, *137*, 67.

[13] Shimon, L. J. W.; Vaida, M.; Addadi, L.; Lahav, M.; Leiserowitz, L. *J. Am. Chem. Soc.* **1990**, *112*, 6215.

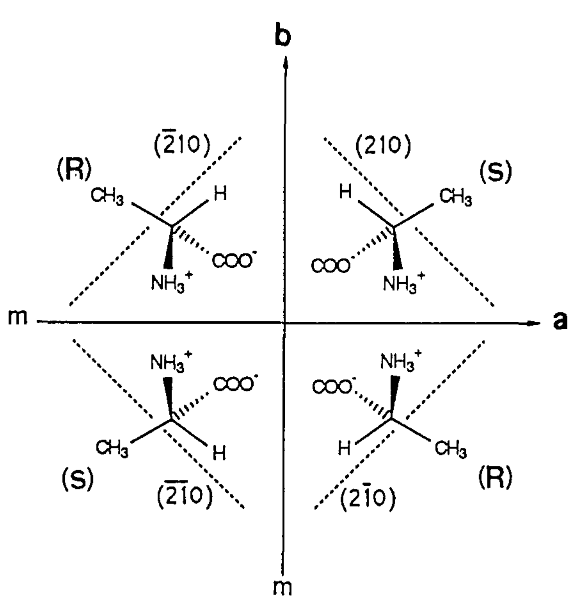

Figure 2. Illustrative representation of the molecular orientations vis-á-vis the four {210} faces in the (*R*,*S*)-alanine crystal as viewed down the *c* axis. At each face only one of the four symmetry-related molecules is oriented such that its C–CH_3 group emerges from the face.

are exposed. Given the absolute sense of the crystal polarity with respect to the *c* axis, the orientation of the *R* and *S* molecules as viewed along the *c* axis are shown in Figure 2. The orientation of the two enantiomeric molecules can be described in terms of their C–CH_3 groups emerging from the {210} side faces. The C–CH_3 groups of the *S* molecules emerge from the (210) and $(\bar{2}\bar{1}0)$ faces, while the methyl groups of the *R* molecules emerge from the $(\bar{2}10)$ and $(2\bar{1}0)$ faces. Thus *S'*-α-amino acid additives can be adsorbed on the (210) and $(\bar{2}\bar{1}0)$ faces and affect their growth, whereas *R'*-α-amino acid additives can be adsorbed and affect the growth of the $(\bar{2}10)$ and $(2\bar{1}0)$ faces.

Induced Twinning of (*R*,*S*)-Alanine Crystals by Optically Resolved α-Amino Acid Additives. In an attempt to obtain induced spontaneous resolution of racemic alanine following the procedure described in Scheme 1, we have grown these crystals in the presence of optically pure α-amino acids threonine or phenylalanine, say of *S* configuration. Instead of resolving the compound as was found in the case of (*R*,*S*)-histidine·HCl, the precipitated crystals proved to be (*R*,*S*)-alanine, assuming a propeller-like shape with the long axis of the propeller parallel to the *c* axis (Figure 3). These crystals exhibit an enantiomorphous morphological symmetry 222 which differs from the *mm*2 achiral morphological symmetry of the pure crystal. On symmetry principles we might have expected the affected crystals to exhibit morphological point symmetry 112, being grown in the presence of the chiral α-amino additive.

One way to account for the 222 morphology of the crystals grown in the presence of optically resolved additives is to assume that the two halves are twinned about the central *ab* plane of the crystal. This would also be in accordance with the fast crystal growth with equal rates at the two opposite ends of the propeller, which is only possible if both ends expose COO^- groups. Here we remind ourselves that in the absence of additive the crystals grow unidirectionally along the polar axis, only at the COO^- end. Close inspection of the crystals showed that the twin parts appear to be stitched together across the middle of the crystal, and are surprisingly attached at "faces" exposing the positively charged NH_3^+ groups. When (*R*,*S*)-alanine was grown in the presence of the α-amino acid additive of opposite handedness, in this case (*R*)-threonine or phenylalanine, the twinned crystals assumed the enantiomorphous morphology. The propeller shape is made manifest not only by the twinned nature of the crystal about its center, but also by the shape of the affected side faces, which are no longer parallel to the *c* axis as they are in the pure form, corresponding to {210}. The affected faces at each side of the crystal were indexed as (21–0.1) and $(\bar{2}\bar{1}$–0.1) when the additive is an *S'*-α-amino acid, and in case the additive is an *R'*-α-amino acid they are $(\bar{2}1$–0.1) and $(2\bar{1}$–0.1). This assignment of the affected faces is understood in terms of the twinning model, where each end of the crystal grows along the −*c* carboxylate end, and the enantioselective binding of the chiral additives to the {210} faces, as described in the previous section. The chiral nature of the propeller arises macroscopically from the fact that the affected pair of side faces, say (21−Δ*l*) and $(\bar{2}\bar{1}-\Delta l)$[14] and the unaffected pair, $(2\bar{1}0)$ and $(\bar{2}10)$, have different areas and slopes. Moreover a cross-sectional (001) cut through each crystal half describes a parallelogram. Had the affected faces remained unchanged of the type {210}, the twinning would not have been immediately obvious.

Scheme 2

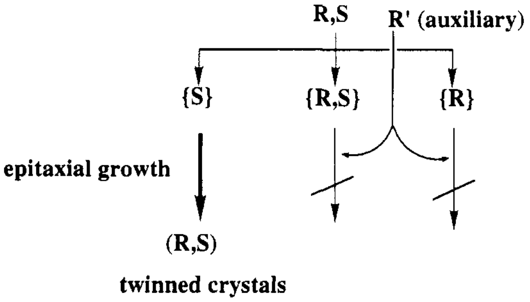

where:
symbols R, R', S and R,S represent molecules
{ } crystalline nuclei
( ) mature crystal

Mechanism of Twinning. To explain this unusual twinning, we propose the following mechanism (Scheme 2). Let us return to the assumption that supersaturated solutions of *R*,*S*-alanine contain a variety of clusters which resemble the corresponding crystals of the (*R*,*S*) and resolved (*R*)- and (*S*)-alanine. The *R'*-α-amino acid additive present in the solution will stereospecifically inhibit growth or even formation of clusters of {*R*,*S*} and {*R*} forms of alanine. Following this hypothesis, the *R'* additive will bind to a lesser extent, if at all, to the {*S*} nuclei, and so should not prevent their growth. We rationalize the formation of (*R*,*S*) twins by assuming that the {*S*} nuclei serve as templates for epitaxial nucleation and growth of (*R*,*S*) crystals by virtue of a particular similarity between the racemic and chiral crystal forms, a fact pointed out by Simpson and Marsh.[15] Following this mechanism, twinning should be avoided when the crystals of alanine are grown in the presence of racemic α-amino acids, as was indeed experimentally observed.

---

[14] The gentle slope of the affected side faces of the twinned crystals indicates Miller indices {21−Δ*l*}, where Δ*l* is very low and found to vary from 0.05 to 0.1, depending on crystallization conditions.

[15] Simpson, H. J.; Marsh, R. E. *Acta Crystallogr.* **1966**, *20*, 550.

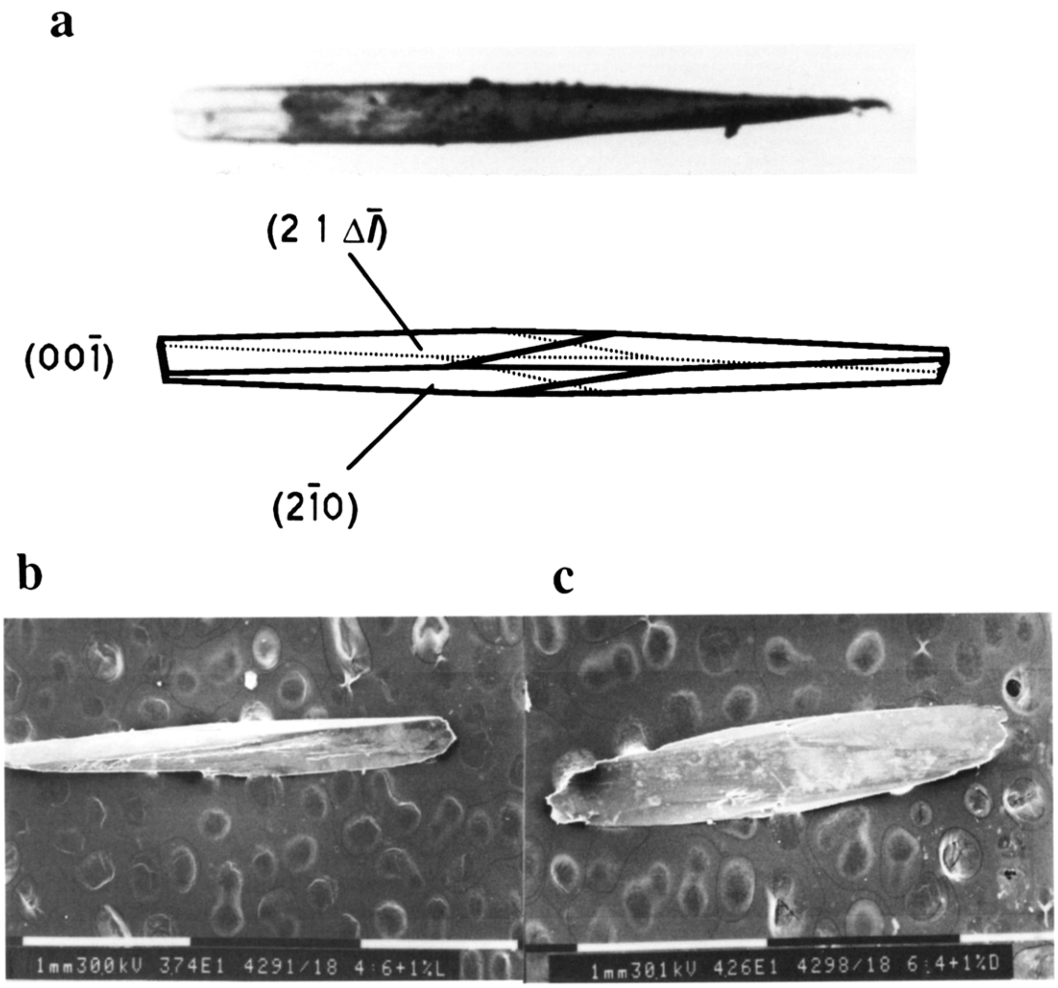

Figure 3. (a) Photograph and computer drawn morphology of (*R*,*S*)-alanine twin crystals grown in the presence of 1% *S*-threonine or *S*-phenylalanine additive. (b) Photograph of twinned alanine crystal grown from solution containing 40:60 *R*:*S* mixture in the presence of 1% *S*-phenylalanine. (c) Photograph of the crystal enantiomorphous to (b) obtained from a 60:40 *R*:*S* mixture grown in the presence of 1% *R*-phenylalanine.

Figure 4 shows the crystalline packing arrangement of (*S*)-alanine[15–17] which belongs to the orthorhombic space group $P2_12_12_1$, with axial dimensions[18] a = 12.32 Å, b = 6.03 Å, c = 5.78 Å, which are almost identical to that of (*R*,*S*)-alanine. The crystal is composed of hydrogen-bonded chains running parallel to the c axis. These chains are interlinked by N–H···O hydrogen bonds about a 2-fold screw axis parallel to the c axis yielding a polar double strand, as in (*R*,*S*)-alanine. These double strands are further interconnected by N–H···O bonds in (*S*)-alanine, generated by 2_1 axes along a (or along b) to yield antiparallel double strands along the c direction. In the (*R*,*S*) form the corresponding hydrogen bonds are generated by n (and so a) glide symmetry so that all double polar strands are parallel along the polar c axis.

As already mentioned the twinned crystals expose CO_2^- groups at the two opposite ends. Thus we focus only on the corresponding epitaxial attachment of the polar crystals of (*R*,*S*)-alanine to the two opposite (001) and (001̄) faces of the chiral (*S*)-alanine nucleus,[19] as depicted in Figure 5. All the hydrogen bonded chains of *S*-alanine molecules parallel to the c axis that emerge from the {001} face of the {*S*} nucleus with their CO_2^- groups exposed at the face maintain the same structure on "conversion" to the racemic crystal. But all those *S*-alanine chains, which are antiparallel to the above and so emerge from the same {001} face with their NH_3^+ groups exposed, must, beyond the interface, be replaced by *R* molecules oppositely oriented vis-á-vis the c axis. Thus across the {001} interface the NH_3^+ groups of the *S* and *R* molecules are directed at each other and separated by about 5 Å as seen in Figure 5.

The *S* chains, which are "converted" into *R* chains at the (001) and (001̄) interfaces of (*S*)-alanine, are related by 2_1 symmetry along the a or b axes in view of the $P2_12_12_1$ symmetry of the chiral crystal. The transformation from the chiral to the racemic phase does not have to occur abruptly at the interface. It may take place gradually along the c axis provided the transformation occurs within each double hydrogen-bonded polar strand whose structure has been described above. In such a way all hydrogen bonds are maintained, except at those points where *S* chains are replaced by *R* chains, and the changes in the van der Waals contacts are minor (Figures 5 and 6). As shall be discussed later, the observed crystals of (*S*)-alanine

---

[16] Dunitz, J. D.; Ryan, R. R. *Acta Crystallogr.* **1966**, *21*, 617.

[17] Destro, R.; Marsh, R. E. ; Bianchi, R. *J. Phys. Chem.* **1988**, *92*, 966.

[18] We have interchanged the a and b axes specified by Simpson and Marsh[15] in order that they be compatible with those of (*R*,*S*)-alanine.

[19] For stereochemical reasons we may expect that (*R*,*S*)-alanine may bind to the {001} faces of (*S*)-alanine such that the ends of the attached (*R*,*S*) crystals would expose NH_3^+ groups, but for kinetic reasons such twinned crystals do not form.

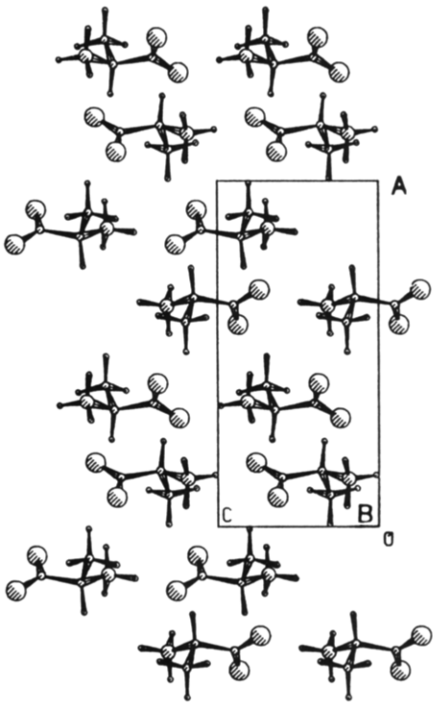

Figure 4. Packing arrangement of (*S*)-alanine viewed along the *b* axis.

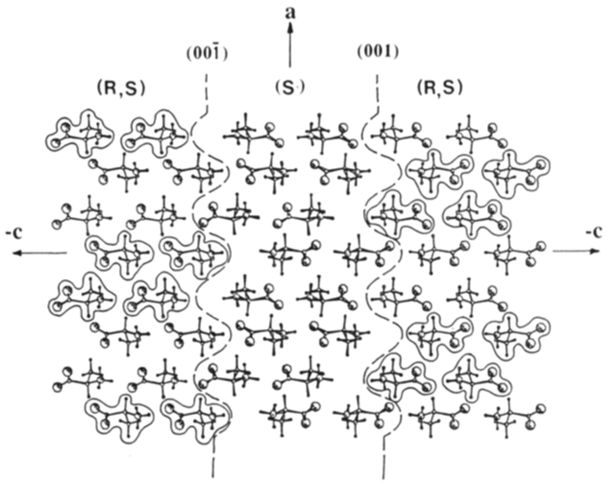

Figure 5. Proposed molecular arrangement of the complex "nucleus" composed of a central {*S*} "nucleus" onto whose (001) and (00$\bar{1}$) "faces" {*R*,*S*}-nuclei have been epitaxially grown. *R* molecules are encircled for clarity. Note that the two {*R*,*S*} "nuclei" are related by 2-fold screw symmetry about the *a* axis of (*S*)-alanine.

do not exhibit {001} faces, at the opposite ends along the *c* axis but rather {101} faces. Nevertheless these faces make an angle sufficiently shallow with respect to the (001) plane that the arguments given in terms of epitaxy at this interface hold. A preliminary test of the feasibility of such an epitaxy was undertaken by growing (*R*,*S*)-alanine at the opposite faces of seed crystals of (*S*) or (*R*)-alanine as shown in Figure 7.

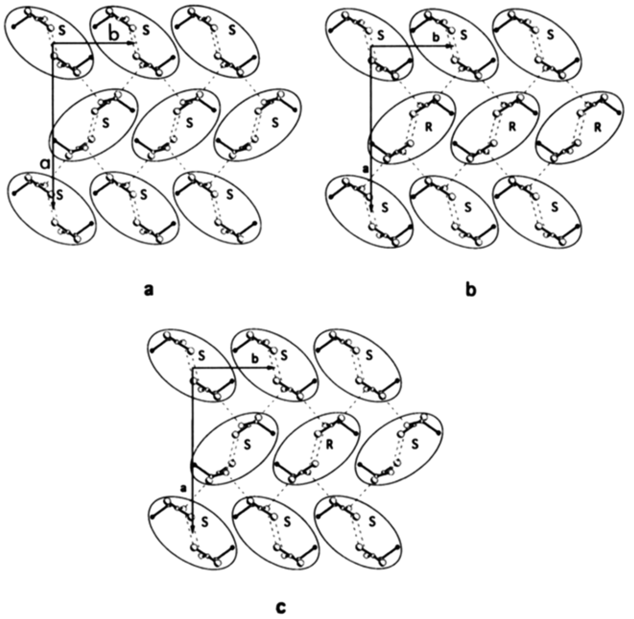

Figure 6. Packing arrangements of alanine viewed along the *c* axis: (a) (*S*)-alanine; (b) (*R*,*S*)-alanine; (c) proposed arrangement of the transitional phase in which one double hydrogen-bonded strand of *S* molecules is replaced by a double *R* strand. The double hydrogen-bonded polar strands along *c*, each enclosed by an ellipse for clarity, describe the two molecular chains interlinked by a 2_1 axis where the molecules in each chain are hydrogen-bonded along *c*.

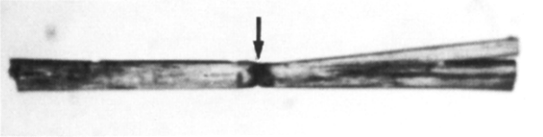

Figure 7. Photograph of crystals of (*R*,*S*)-alanine epitaxially grown at the opposite sides of an (*S*)-alanine seed.

To obtain further insight on the twinning phenomenon, we tried to probe the structure of the twinned parts by a variety of techniques. All attempts made to detect the presence of enantiomeric excess of *S*-alanine from the twinned zone of the crystals grown in the presence of *R*′-α-amino acid additives, were unsuccessful. We were unable to detect circular dichroism of the copper complex of alanine or obtain any enantiomeric excess, using gas chromatography (GC) on a capillary chiral column. On the other hand, structural information suggestive of a chiral nucleus embedded within the twinned zone could be obtained by X-ray diffraction measurements, from the reflections which are symmetry forbidden in the pure (*R*,*S*) crystal, as shall be described.

Characterization of the Twinned Crystals by Electron Microscopy. Various twinned crystals were examined by scanning electron microscopy (SEM). Each of the specimens showed a narrow crack along the perimeter in the middle of the twinned crystal, separating the two propeller halves. These cracks formed a zigzag pattern approximately perpendicular to the polar *c* axis (Figure 8). Assuming the proposed mechanism of epitaxial growth, we may reasonably deduce that the starting nucleus is located somewhere inside this crack. The approximate width of the crack was 1.5 μm. Assuming a cube-shaped "nucleus" of this dimension, would lead to a volume of 4 $\times 10^{-9}$ mm^3 compared with the typical volume of the crystal of ~0.3 × 0.3 × 3 mm = 0.3 mm^3. Thus the volume of this deduced "nucleus", located in the crack, is 8 orders of magnitude smaller than the mature crystal.

The structural source of the perturbation leading to the formation of these cracks is not completely clear. We know from X-ray diffraction measurements on some twinned specimens (see below), that the two propeller halves are not completely aligned; there is a shear angle of about 0.7° between their *ab* planes. Whether the distortion arises

Figure 8. SEM photograph of the crack in a twinned (*R,S*) crystal. The *c* axis of the crystal is indicated.

from a mismatch between the cell dimensions of the chiral nucleus and the racemic crystal or because of repulsion between the exposed NH_3 groups of the two epitaxially grown halves at their (001) "faces" as they eventually "meet", is not clear.

X-ray Diffraction Analysis of Twinned Crystals. The deduction that the twinned crystals of (*R,S*)-alanine consist of a central nucleus of one of the enantiomorphs, from which two ends the two halves of the (*R,S*) crystal grew, is supported by X-ray diffraction measurements.

A propeller-shaped crystal specimen of dimensions 0.1 × 0.1 × 0.8 mm was mounted on the diffractometer along the *c* axis, the direction of crystal elongation. Several reflections measured with a standard collimator,[20] of diameter 1 mm, so that the whole crystal was bathed in the X-ray beam, yielded split diffraction profiles indicating two crystal halves (Figure 9a). Adjustment of the height of the crystal so that only each of its two crystal halves were separately irradiated, yielded regular diffraction profiles corresponding to a single crystal (Figure 9b). The precise orientation of each of the two halves was determined. Misalignment between the two halves occurs primarily in the *ab* plane with a "twist" angle of about 0.7° whereas the misalignment angle along the propeller *c* axis is about 0.3°. This result is in keeping with the observation that the two crystal halves appear stitched together across the central plane (Figure 8).

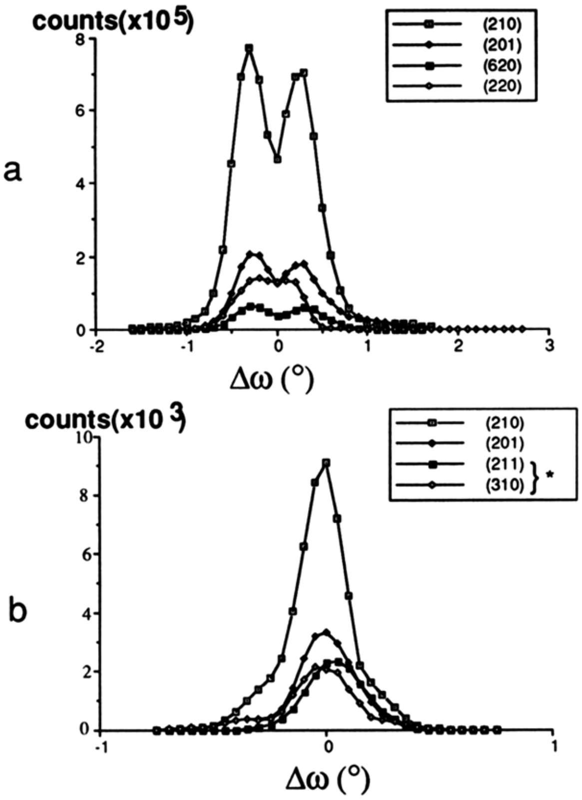

* Intensity is multiplied by factor 10

Figure 9. ω-scans measured for some general reflections of a twinned (*R,S*)-alanine crystal specimen: (a) scans taken from the whole crystal using a wide collimator; (b) scans taken from a tip of the crystal using a narrow collimator. Note that in an ω-scan the X-ray detector is kept at the Bragg 2*θ* angle, and the crystal is rotated around its diffracting position.

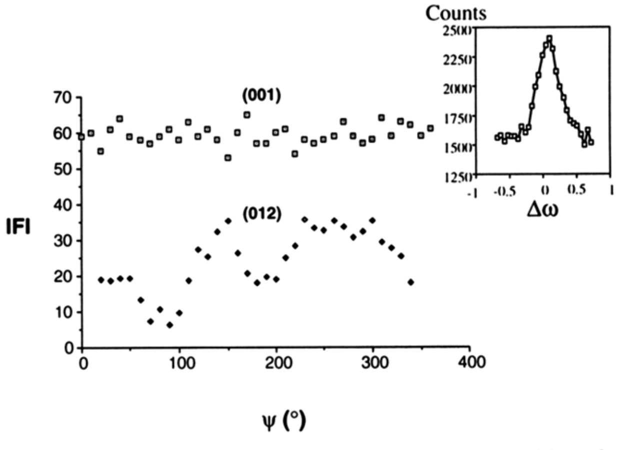

Figure 10. *ψ*-scans for the (001) and (012) reflections. Note that in a *ψ*-scan the X-ray detector is kept at the Bragg 2*θ* angle, the crystal is always in diffraction position and is rotated around its diffracting vector $d^*_{(hkl)}$; in this case (*hkl*) being (001) or (012). Note that |*F*| corresponds to the magnitude of the observed structure factor $|F| = K(I-B)^{1/2}$, where *I* is the integrated intensity of the reflection, *B* is the background, and *K* a geometrical factor. The insert shows an *ω* scan of the (001) reflection for a particular value of *ψ*, indicating a definite diffraction peak.

A "nucleus" with a crystal structure similar to that of (*R*)- or (*S*)-alanine in space group $P2_12_12_1$ implies that only X-ray reflections of the type $h00$, $0k0$, $00l$, $h,k,l = 2n + 1$ should be absent on symmetry grounds. On the other hand, the symmetry-forbidden reflections for the two crystal halves of space group $Pna2_1$ are $0kl$, $k + l = 2n + 1$ and $h0l$, $h = 2n + 1$. Making use of a narrow X-ray beam collimator[21] of diameter 0.1 mm, the symmetry-forbidden reflections were measured from the twinned crystal separately irradiated at its center and two ends. Only two reflections, the (012) and (001), coming only from the crystal center, had significant net intensities. To preclude the possibility of multiple X-ray diffraction *ψ* scans were measured for these two reflections (Figure 10). Moreover *ω*-scans were made for the (012) reflection at 12 different *ψ* values (Figure 11). From these results there can hardly be any doubt as to the presence of the two reflections. Table 1 lists the strongest calculated structure-factor |*F*(*hkl*)| values for the crystal structures of (*R,S*)-alanine

---

[20] The cross-sectional diameter of the beam illuminating the crystals was about 1 mm for the 1-mm collimator. Here we note that a graphite crystal was used as a monochromator for the X-ray beam.

[21] We did not measure the cross-sectional diameter of the beam illuminating the crystal but, since the diameter of the beam with the wide collimator was approximately 1 mm, we could deduce that the beam was considerably reduced in intensity. Note that the ratio of intensities of the (210) reflection measured with the wide and narrow colimators was in the range 100, in keeping with the relative areas of the two collimators (see Figure 9).

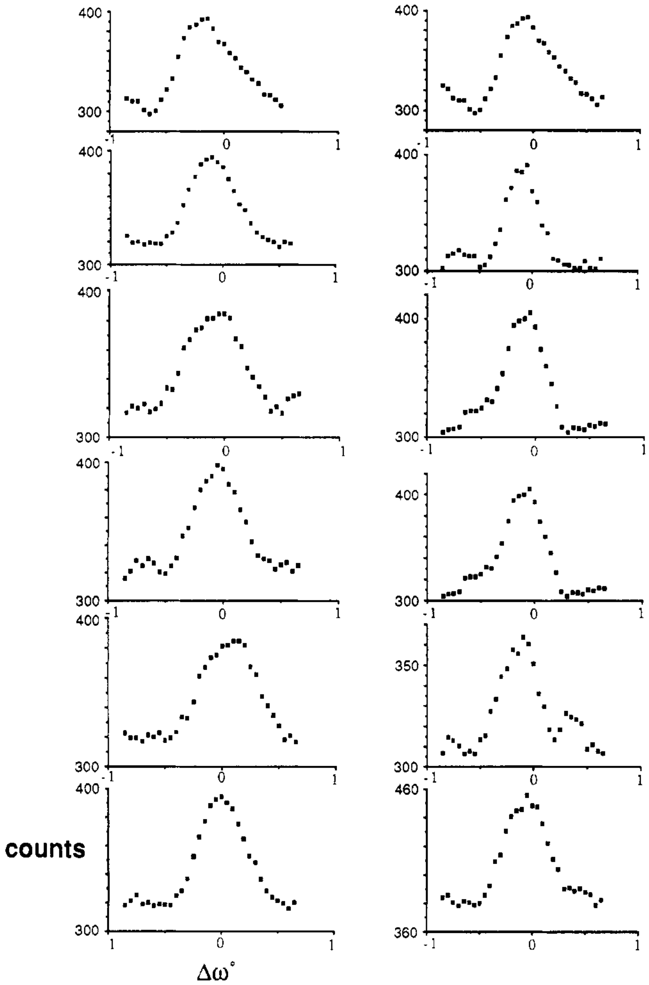

Figure 11. ω-scans measured for the (012) reflection at 12 different ψ-orientations of the crystal ranging from 0 to 360° in steps of 30°.

Table 1. Strongest Calculated Structure Factors for the Crystal Structures of (*R*,*S*)-Alanine and (*S*)-Alanine

(*R*,*S*)-alanine		(*S*)-alanine	
hkl	|*F*|	*hkl*	|*F*|
210	100	210	101
400	93	400	91
002	68	002	65
201	55	*012*[a]	64
410	52	410	49
112	51	620	49
620	48	220	48
220	46	311	42
311	39	*101*[a]	41
011	32	412	39
402	30	*301*[a]	36

[a] Reflections which are symmetry forbidden in (*R*,*S*)-alanine.

and (*S*)-alanine. The (012) reflection, which is symmetry-forbidden for (*R*,*S*) alanine, has one of the highest $|F(hkl)|$ values in the list for (*S*)-alanine. Therefore, on the basis that the measured intensity of the (012) reflection comes from a $P2_12_12_1$ nucleus of chiral alanine we have been able to derive its crystal volume. For this purpose we made use of the measured volume of the twinned crystal, coupled with a knowledge of the relative diffraction intensities from the two crystalline phases of alanine. Assuming the crystal nucleus of alanine is cubic in dimension, the calculated length[22] of each side is 5 μm. To obtain significant intensities from such a small "crystal", advantage was taken of the high X-ray flux from the 18-kW rotating anode X-ray generator as well as long measuring times. The length of 5 μm is of the same order of magnitude as the width of the "stitched" crack across the center of the specimen crystal measured by electron scanning microscopy (Figure 8).

Table 2. Crystal Form and Composition Obtained by Crystallization from Supersaturated Solutions of Various *R*:*S* Compositions

solution composition (*R*:*S*)-alanine	crystal form	crystal composition[a] % *R*	% *S*	remarks
50:50	*R*,*S* needles	50	50	
40:60	*R*,*S* twinned	48	52	middle part 45:55
60:40	*R*,*S* twinned	51	49	
35:65	*R*,*S* twinned	47	53	
65:35	*R*,*S* twinned	51	49	
30:70	*S* + *R*,*S* polycrystals	36	64	
25:75	*S* + *R*,*S* polycrystals	28	72	middle part 30:70 end parts 26:74
22:78	*S* + *R*,*S* polycrystals			
20:80	*S* + *R*,*S* polycrystals	10	90	
17:83	*S* + *R*,*S* polycrystals	8	92	middle part 5:95 end parts 10:90
15:85	affected *S* crystals	0.7	99.3	

[a] Estimated error in composition is about 1%.

There remains, however, the problem of accounting for the presence of the (001) reflection which is symmetry forbidden for the space groups of both (*R*,*S*)-alanine ($Pna2_1$) and chiral alanine ($P2_12_12_1$). The presence of the (001) reflection indicates a loss of the 2-fold screw axis along the *c* axis. A simple way to rationalize the loss of this symmetry element is to assume that the structural transition from $P2_12_12_1$ to $Pna2_1$ is gradual as described above. We had postulated that the transition from (*S*)-alanine to (*R*,*S*)-alanine involves a random replacement of *S*-alanine hydrogen-bonded double strands parallel to *c*, by the corresponding *R*-double strands (see Figure 6). In this way, the 2-fold screw symmetry along *c* would be partially lost for the intermediate disordered region. We cannot, however, make a qualitative estimate of the effect of such disorder on the intensity of the (001) reflection.

Induced Twinning of (*R*,*S*)-Alanine Crystals Grown from Chiral Nonracemic Mixtures of Alanine. Additional support for the proposed twinning mechanism was provided by growth of single crystals of (*R*,*S*)-alanine from enantiomerically enriched solutions. The presence of say excess *R*-alanine will generate higher concentrations of {*R*} nuclei as templates for the growth of the twinned crystals. Indeed, when crystals were grown from supersaturated solutions of enantiomeric *R*:*S* ratios in the range from 45:55 to 35:65, twinned crystals with propeller-like shape were obtained. The enantiomeric composition of these crystals was determined by GC, and the results showed an *R*:*S* ratio for all the specimens, fluctuating around a value of 50:50.

The composition of the middle zone of the twinned crystals was also examined by GC. Crystals grown from supersaturated solutions of a 40:60 *R*:*S* ratio contained a 45:55 *R*:*S* composition of alanine in the middle zone (Table 2). The presence of an excess of the *S* enantiomer, in the twinned zone supports our proposed mechanism that the nucleus of the twinned crystals must be *S*-like.

---

(22) An (*S*)-alanine "nucleus" of volume ~100 μm^3 which is approximately 10^{-10} g would not be detectable by GC, being overwhelmed by the amount of material of ~0.1 – 1 mg cut from the *R*,*S* crystal. Regarding the CD measurements, the estimated amount of material from the nucleus is well below the threshold detection limit of the instrument used.

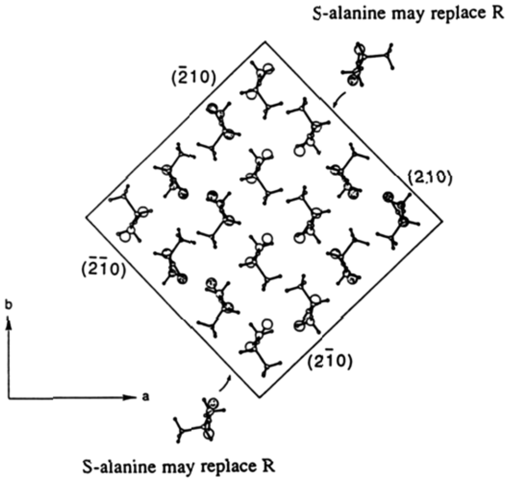

Figure 12. Packing arrangement of (*R*,*S*)-alanine viewed down the *c* axis, delineated by the (210) and $(\bar{2}\bar{1}0)$ faces, showing where adsorbed (*S*)-alanine molecules may replace *R*-molecules. Note that at each face only one of the four symmetry related molecules has its C(chiral)–H bond emerging from the face. The dark molecules are *S*-alanine. The N(amino) atom has a larger circle than the C(methyl) atom.

The 40:60 *R*:*S* alanine mixture in solution gave the same enantiomorphous propeller-shape of the twinned crystals as a 50:50 mixture in the presence of *S*-phenylalanine additive. This result can be understood in terms of two consecutive growth mechanisms: The first involves twinning starting from a chiral nucleus arising from a local excess of *S*-alanine followed by epitaxial growth of (*R*,*S*)-alanine. The second involves formation of the propeller shape which can be understood in terms of replacement of *R* molecules by *S*-alanine molecules at the (210) and $(\bar{2}\bar{1}0)$ faces, as shown in Figure 12. This replacement can take place because of an interchange of a hydrogen atom by an CH_3 group (Figure 12). Note that the *S*-phenylalanine additive replaces an *S*-alanine molecule on the same face as *S*-alanine replaces *R*-alanine. Crystallization from solutions containing a combination of 40:60 *R*:*S* mixture and 1% *S*-phenylalanine yielded the regular propeller-shape crystals (Figure 3b). An enantiomorphous morphology (Figure 3c) was obtained with the 60:40 *R*:*S* and 1% *R*-phenylalanine. But 1% *R*-phenylalanine addition to the solution containing 40:60 *R*:*S* mixture resulted in almost powder-like crystals where all side faces were affected.

Crystals were also grown from supersaturated solutions containing the *R*:*S*-alanine ratios varying from 35:65 to 0:100 (Figure 13 and Table 2). Supersaturated solutions with a *R*:*S* ratio of 35:65 yielded (*R*,*S*) twinned crystals of composition close to 50:50, and a solution composition of 15:85 gave affected (*S*)-alanine crystals (Figure 13) containing minor amounts of *R*-alanine. Solutions with *R*:*S* ratios 30:70, 25:75, and 20:80 yielded polycrystals displaying an unusual morphology incorporating both the shape of the (*R*,*S*) twin form and that of the (*S*)-alanine (Figure 13). The pure (*S*)-alanine crystals exhibit well-developed faces of type {210}, {110}, and, at the opposite ends along the *c* axis, {101} faces (Figure 13e). These crystals become elongated in *c* on growth in the presence of the opposite enantiomer (Figure 13d).[23]

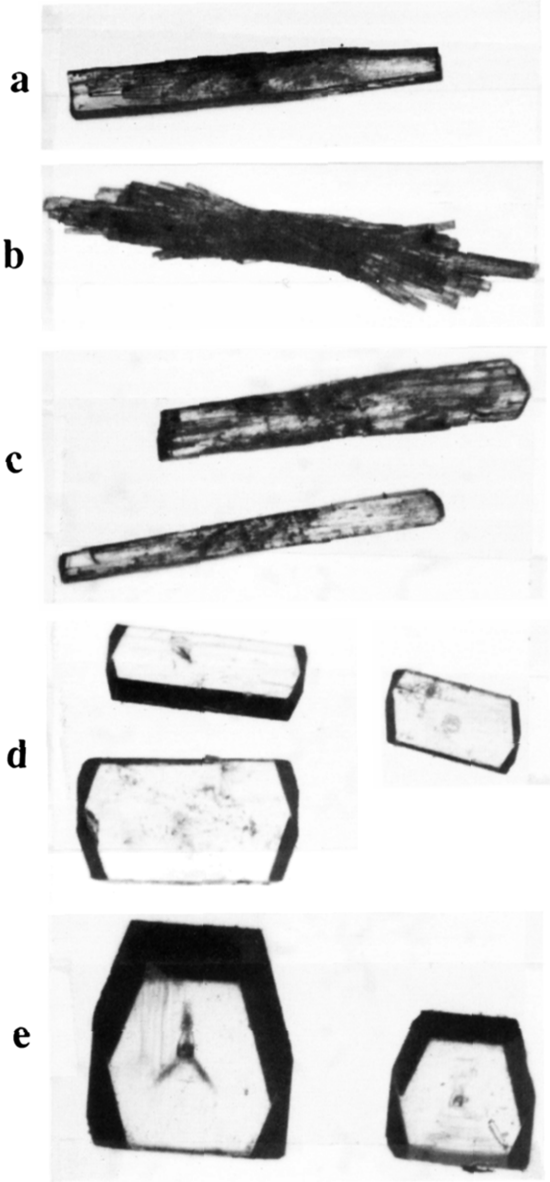

Figure 13. Photographs of crystals grown from supersaturated solutions containing alanine of various enantiomeric *R*:*S* ratios: (a) 35:65; (b) 25:75; (c) 20:80; (d) 15:85; (e) 0:100.

Solutions containing 17:83 *R*:*S* mixtures yielded polycrystalline material of racemic and chiral forms. Optical resolution was nevertheless achieved by addition of 1% *R*-phenylalanine to these solutions. This result indicates that the growth of both {*R*} and {*R*,*S*} nuclei into stable crystals are inhibited. Furthermore, the result is similar to the optical resolution of *R*,*S* histidine·HCl,[5] in the sense that the chiral additive inhibited formation of both the racemic as well as the chiral form homomeric to the additive.

X-ray Diffraction Analysis of a Twinned Crystal Grown from a 40:60 *R*,*S* Mixture. A twinned propeller-shaped crystal of alanine grown from a 40:60 *R*:*S* mixture of dimensions 0.6 × 0.1 × 1.1 mm was explored by X-ray diffraction. When the whole crystal was bathed in the X-ray beam, it yielded observable intensities for many of the reflections forbidden by space group $Pna2_1$. The same behavior was observed when only the crystal center or its ends were irradiated using a narrow X-ray beam. These results pointed to a pronounced reduction in symmetry throughout the whole crystal.[24–28]

---

[23] We note that Simpson and Marsh[15] reported needlelike crystals of (*S*)-alanine exposing {110} side faces when grown from aqueous solution.

Table 3. Crystallographic Data for (*R,S*)-Alanine Twinned Crystals

	crystal grown from 50:50 *R*:*S* and 1% *S*-phenylalanine	(*R,S*)-alanine grown from a 40:60 *R*:*S* mixture	
temperature/K	290	290	100
space group	$Pna2_1$	$P1$	$P1$
formula	$C_3H_8NO_2$	$C_3H_8NO_2$	$C_3H_8NO_2$
a/Å	12.025(3)	12.019(3)	11.895(2)
b/Å	6.041(2)	6.032(2)	5.964(1)
c/Å	5.829(2)	5.828(2)	5.826(2)
α/deg	90.00(3)	90.01(3)	89.98(2)
β/deg	90.02(3)	90.03(2)	90.04(2)
γ/deg	89.99(3)	89.76(2)	89.67(1)
V/Å^3	423.5	422.5	413.9
z	4	4	4
X-radiation	Cu Kα (1.5418 Å)	Cu Kα (1.5418 Å)	Cu Kα (1.5418 Å)
crystal size × 10 (mm)	1 × 1 × 8	6 × 1 × 6	6 × 1 × 6
no. of reflections[a]			2675

[a] Intensities of X-ray reflections forbidden for $Pna2_1$ space group were measured at speeds 8 times slower than the "normal" reflections.

Table 4

(a) Laue Symmetry	2/*m*2/*m*2/*m*	2/*m*11	12/*m*1	112/*m*
$R_m(F^2)$[a]	0.068	0.090	0.089	0.046
no. of "independent reflections[b]	399	654	685	685

(b) space group	$Pna2_1$	$Pn11$	$P1a1$	$P112_1$
no. of observed "symmetry-forbidden" reflections ⟨$F/\sigma(F)$⟩[c]	184 3.2	58 4.3	126 2.8	6 7.0

[a] $R_m(F^2) = \sum|F^2 - F_i^2|/\sum F_i^2$, where F^2 is the average of the set of observed symmetry-related structure factors and F_i^2 is the *i*th individual observed structure factor. [b] Note that the number of "independent" reflections depends upon the Laue symmetry assignment. [c] ⟨$F/\sigma(F)$⟩ is the average value of the ratio of F_{obs} divided by $\sigma(F_{obs})$.

To determine the crystal structure by X-ray diffraction, measurements were made on only one-half of the propeller (0.6 × 0.1 × 0.6 mm) which was cut from the specimen crystal. In this way we avoided a masking of the reduction in lattice symmetry that would have been imposed by crystal twinning about the central *ab* plane. The specimen crystal was cooled to a temperature of ~100 K for the X-ray diffraction measurements in order to facilitate structure determination. Cell dimensions and information on X-ray diffraction data collection are given in Table 3.

Evidence in favor of crystal symmetry lowering was obtained from the following results. The unit-cell dimensions (Table 3) indicates a monoclinic cell, with *c* as the unique axis since the angle γ deviates significantly from 90°, unlike the α and β values. This effect cannot be due to the reduction in crystal temperature, since the unit-cell angles at room temperature followed the same pattern.

Reflections within a hemisphere of reciprocal space out to sin θ/λ of 0.56, were measured (Table 3). The agreement factor, $R_m(F^2)$, between the intensities of symmetry-related reflections assuming crystal point symmetries 2/*m*2/*m*2/*m*, 2/*m*11, 12/*m*1, and 112/*m* (Table 4a) favors 112/*m*, indicating monoclinic symmetry with *c* as the unique axis.

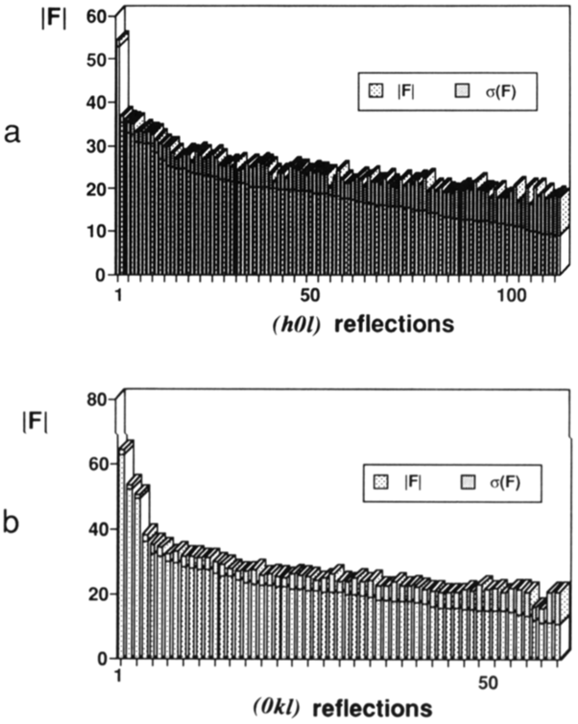

Figure 14. Observed structure factor $|F_{(hkl)}|$ values of symmetry-forbidden (for space group $Pna2_1$) reflections for the (*R,S*)-alanine crystal grown from 40:60 *R*:*S* mixture; (a) (*h*0*l*) reflections, $h = 2n + 1$; (b) (0*kl*) reflections, $k + l = 2n + 1$.

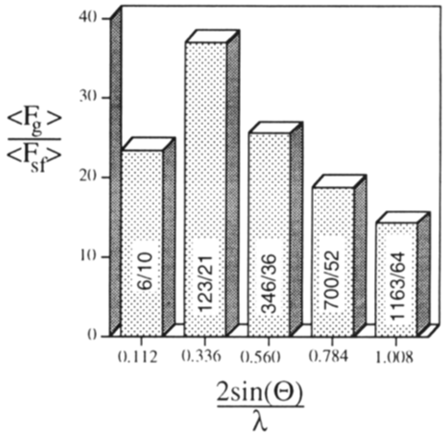

Figure 15. Ratio of the average values of F_{obs} for general $<F_g>$ and "symmetry-forbidden" reflections $<F_{sf}>$ in shells of reciprocal space (2 sin θ)/λ. Also given are the number of general *hkl* reflections vs the number of "symmetry-forbidden" reflections.

This result is in agreement with the unit cell dimensions. Furthermore the *n* and *a* glide planes, that appear in pure (*R,S*)-alanine, are lost since the X-ray reflections forbidden by these two symmetry elements are indeed observed (Figure 14 and Table 4b). The intensities of these "symmetry-forbidden" reflections were much weaker than the general reflections *hkl*, according to the histogram given in Figure 15. The loss of the *n* and *a* glide planes does not however negate the presence of a 2-fold screw axis along the *c* direction. The loss of the 2_1 axis along *c* is evident from the presence of the weak X-ray reflections 00*l*, $l = 2n + 1$ (see Table 4b). At this point we stress that the twinned crystal of (*R,S*)-alanine grown from a racemic solution but in the presence of the additive *S*-phenylalanine, described in the previous section, did not show the presence of symmetry-forbidden reflections, but for (001) and (012) only in the middle zone of the crystal. This

---

(24) Vaida, M.; Shimon, L. J. W.; Weissinger-Lewin, Y.; Frolow, F.; Lahav, M.; Leiserowitz, L.; McMullan, R. K. *Science* **1988**, *241*, 1475.

(25) Gopalan, P.; Peterson, M. L.; Crundwell, G.; Kahr, B. *J. Am. Chem. Soc.* **1993**, *115*, 3366.

(26) McBride, J. M.; Bertman, S. B. *Angew. Chem., Int. Ed. Engl.* **1989**, *28*, 330.

(27) Allen, F. M.; Buseck, P. R. *Am. Mineral.* **1988**, *73*, 568.

(28) Shimon, L. J. W.; Vaida, M.; Frolow, F.; Lahav, M.; Leiserowitz, L.; Weissinger-Lewin, Y.; McMullan, R. K. *Faraday Discuss.* **1993**, *95*, 307.

crystal and the specimen grown from a solution containing 40:60 R:S mixture were of approximately the same size. The diffraction data of the specimen crystal grown from the 40:60 R:S mixture still leave, however, for an ambiguity in pinpointing the space group of the structure.

We may resolve this question in the following way. We try to rationalize the reduction in symmetry in terms of the affected crystal morphology and given the fact that the crystals grown from a 40:60 R:S solution contain only 1–2% excess of occluded S enantiomer, according to GC analysis. The two affected side faces of the cut prismatic crystal were of the type $(21{-}\Delta l)$ and $(\bar{2}\bar{1}{-}\Delta l)$; the other two faces $(2\bar{1}0)$ and $(\bar{2}10)$ remained unchanged, as in pure (R,S)-alanine. This morphology is compatible with the adsorption of S-alanine molecules at particular R type sites on the affected faces (Figure 12). An S-alanine molecule can only occupy an R type surface site on the affected faces without incurring repulsive intermolecular contacts if the C–CH_3 group emerges from the face. Consequently only one of the four crystallographically different surface sites on the affected $\{21{-}\Delta l\}$ faces may be partially occupied by S-alanine molecules replacing regular R molecules. Occlusion of such S molecules would lead to a reduction in crystal symmetry to $P1$. The two structures, resulting from occlusion through the $(21{-}\Delta l)$ and $(\bar{2}\bar{1}{-}\Delta l)$ faces are not identical but rather related by 2-fold screw symmetry, in keeping with the fact that the affected sites on the $(21{-}\Delta l)$ and $(\bar{2}\bar{1}{-}\Delta l)$ faces are related by 2_1 symmetry. Since the crystal may be regarded as composed of mosaic blocks diffracting independently, the X-ray intensity contribution to each (hkl) reflection comes from two crystal structures, each of symmetry $P1$, but related to each other by 2-fold symmetry about the c axis. Thus the prismatic crystal may be regarded as composed of two $P1$ sectors, related by 2-fold point symmetry, coherently intertwinned about the central (210) plane that intersects the two halves of the prism. In this way we may account for the monoclinic character with c as the unique axis of the cut prismatic crystal.

The crystal structure was first refined assuming the space group $Pna2_1$ with anisotropic temperature factors for the C, N, and O atoms. The H atoms were located by difference Fourier syntheses in their expected positions. Further refinement with fixed H-atoms positions, and a common isotropic temperature factor for all H-atoms yielded a reliability index $R(F) = 0.035$ for all the symmetry permitted reflections averaged according to the Laue point symmetry mmm. The $R(F)$ factor calculated for Laue point symmetry $\bar{1}$ (namely, without averaging the symmetry-related reflections) was 0.065. Including the symmetry-forbidden reflections ($0kl$, $k + l = 2n + 1$; $h0l$, $h = 2n + 1$) had a minor effect on this agreement factor. The $R(F)$ index of 0.035 is low and would, at first sight, indicate that the $Pna2_1$ assignment of the space group is correct. But all the observed data and analysis described above rules out this possibility unambiguously. Thus we searched in the difference Fourier synthesis for evidence of enantiomeric disorder in the crystal. The four strongest peaks in the resulting Fourier difference map were close to the oxygen atoms, in the region where lone pair density is expected to be. The fifth strongest peak lay in the direction of the C(chiral)–H vector at a distance of about 1.5 Å from the C(chiral) atom position. This peak corresponds to a methyl carbon atom at an enantiomerically disordered molecular site, in terms of the arguments on molecular adsorption outlined above. Therefore we constructed a crystal structure in which the unit cell was composed of two ordered S-type sites, one ordered R-type site and the remaining R-type site occupied by a composite molecule consisting of primarily R mixed with an S molecule.[29] We naturally assumed that the conformation of the S molecule was such that its CO_2^- and NH_3^+ groups coincided with that of the dominant R species. The space group of this structure is $P1$. We took care of the crystal "twinning" about the central (210) plane by combining the calculated intensity contributions of the (hkl) and ($\bar{h}\bar{k}l$) reflections. Refinement which involved only the linked occupancy of the CH_3 and H groups at the disordered sites, as a parameter, yielded for the S molecules an occupancy of 0.020(4). Only the symmetry-forbidden reflections were used to determine the occupancy, whose value corresponds to an average of 50.5% S molecules in the overall crystal. The final $R(F)$ index was 0.43. The match between the observed and calculated $|F|$ values for all these "symmetry-forbidden" reflections is shown in Figure 16. Clearly, the model, in which the H and CH_3 groups are interchanged for the composite molecule at the site of occlusion, does not yield a good fit between the F_{obs} and F_{calc} for the "symmetry-forbidden" reflections. We did not take into account a concerted rearrangement of the molecules in the vicinity of the site of disordered occlusion arising from very short intermolecular contacts (Figure 17). Indeed we propose that this rearrangement must be a regular feature at the occlusion sites within the diffracting domains, in order to account for the presence of the

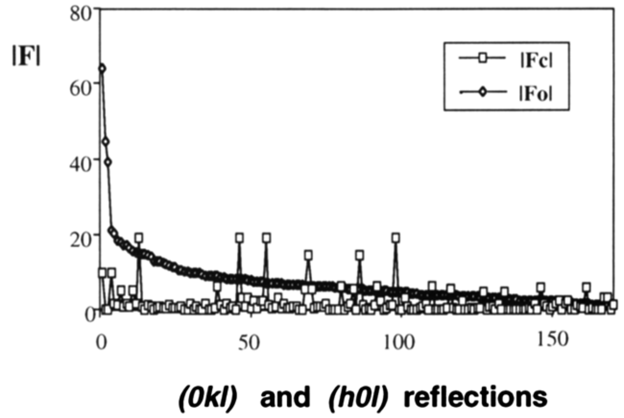

Figure 16. Observed (◊) and calculated (□) structure factors F_{hkl} for the "symmetry-forbidden" reflections $0kl$, $k + l = 2n + 1$ and $h0l$, $h = 2n + 1$.

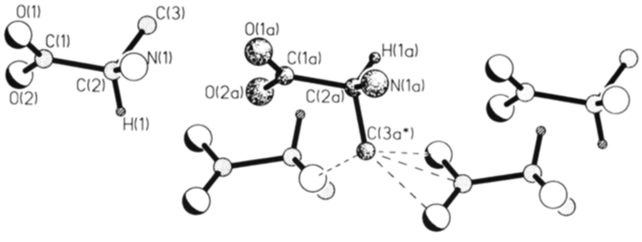

Figure 17. Short intermolecular contacts about a disordered site in the crystal. The dark molecule represents a S-alanine occupying a crystallographic R site. The short C(3a*)···N(1), C(3a*)···O(2), C(3a*)···C(1) and C(3a*)···O(1) distances are 2.7, 2.8, 2.6, and 2.2 Å respectively.

---

[29] This assumption is in keeping with the observed change in crystal morphology of chiral resolved N-cinnamoylalanine grown in the presence of its enantiomer (Berkovitch-Yellin, Z.; Addadi, L.; Idelson, M.; Leiserowitz, L.; Lahav, M. *Nature* **1982**, *256*, 27).

symmetry-forbidden reflections and the observed Laue symmetry. Moreover, this model implies that the enantiomeric disorder occurs within the crystal bulk[30] rather than on the surfaces of mosaic blocks. This system, of reduced crystal symmetry, differs from two host-additive organic systems with reduced crystal symmetry studied by X-ray and neutron diffraction[31] in two main respects: the latter contained relatively high amounts of occluded additive (>8%) which caused only minor perturbation of the normal intermolecular contacts.

Conclusion

We have provided information on the structure of nuclei formed at very early stages of the crystallization process. The unusual shape of the enantiomorphous twins of (*R*,*S*)-alanine induced by the chiral α-amino acid additives is prima facie evidence that the clusters, at very early stages of their formation, assume structures akin to their mature crystalline phases. In systems where more than one crystalline phase can be formed, additive molecules designed on the structural basis of the mature crystal can be targeted stereospecifically to particular nuclei resulting in a prevention of their growth into macroscopic crystals. The present results demonstrate that the "tailor-made" additive is a far more efficient inhibitor during the stage of crystal nucleation than during the later stage of crystal growth. But once the nuclei of the phase unaffected by the additive reached a certain size, it acted as a template for the epitaxial crystallization of the thermodynamically more stable form, leading to unusual twinning of the crystal of (*R*,*S*)-alanine. The "tailor-made" auxiliary can reduce the speed of growth of the faces it interacts with and modify the morphology of the crystal, but hardly can prevent the crystal formation. The X-ray intensity diffraction pattern of a twinned crystal of (*R*,*S*)-alanine grown from 40:60 *R*:*S* alanine solutions indicated symmetry lowering as a result of enantiomeric disorder.

The present studies also have bearing on theoretical aspects of crystal nucleation. The existence of structured clusters in supersaturated solutions prior to crystal nucleation invokes again the central role played by the anisotropy in intermolecular forces in the organization of molecules and raises the question whether the importance of interfacial effects have not been overstated in classical theories.[33,34]

Recent studies have been made on the self-organization of amphiphilic and bolaamphiphilic molecules at air–solution interfaces into crystalline monolayers and multilayers[35,36] of three-to-five layers thick. The ability to observe their structure and follow their dynamics as affected by "tailor-made" additives by modern methods such as grazing incidence X-ray diffraction, complemented by atomic force microscopy and cryo-transmission electron microscopy, should provide a more direct entry in the understanding of the mechanism of growth, dissolution and microtwinning of clusters at the early stages of crystal nucleation.

Acknowledgment. We acknowledge the help of Eli Friedman. We thank the Israel Academy of Basic Sciences and Humanities for financial support.

---

(30) The diffraction results obtained on the specimen crystal grown from 40:60 *R*:*S* mixture in solution raises the question whether occasional enantiomeric disorder does not occur by the same mechanism of adsorption and occlusion in the case of a crystal grown from racemic solution. As already mentioned, the X-ray diffraction results obtained from the twinned crystal of (*R*,*S*)-alanine grown from a 50:50 mixture but in the presence of 1% *S*-phenylalanine did not show the presence of symmetry-forbidden reflections beside the (001) and (012) in the middle zone of the crystal.

(31) The two host-additive systems studied were asparagine-aspartic acid[32] and cinnamamide–thienylacrylamide.[24,28]

(32) Weissinger-Lewin, Y.; Frolow, F.; McMullan, R. K.; Koetzle, T. F.; Lahav, M.; Leiserowitz, L., *J. Am. Chem. Soc.* **1989**, *111*, 1035.

(33) Larsen, M. A. In *Advances in Industrial Crystallization*, Butterworth-Heinemann Ltd.: London, 1991, p 20.

(34) Peters, G. H.; Eggebrecht J.; Larsen, M. A. *Proceedings of the 11th Symposium on Industrial Crystallization*; Mersmann, A., Ed., Garmisch, Germany, 1990; p 883.

(35) Popovitz-Biro, R.; Majewski, J.; Margulis, L.; Cohen, S.; Leiserowitz, L.; Lahav, M. *J. Phys. Chem.* **1994**, *98*, 4970.

(36) Weinbach, S.; Kjaer, K.; Grübel, G.; Legrand, J.-F.; Als-Nielsen, J.; Lahav, M.; Leiserowitz, L. *Science* **1994**, *264*, 1566.